

# Differential cross section and photon-beam asymmetry for the $\bar{\gamma}p \rightarrow \pi^- \Delta^{++}(1232)$ reaction at forward $\pi^-$ angles for $E_\gamma=1.5-2.95$ GeV

H. Kohri,<sup>1,2</sup> S. H. Shiu,<sup>2,3</sup> W. C. Chang,<sup>2</sup> Y. Yanai,<sup>1</sup> D. S. Ahn,<sup>4</sup> J. K. Ahn,<sup>5</sup> J. Y. Chen,<sup>6</sup> S. Daté,<sup>7</sup> H. Ejiri,<sup>1</sup> H. Fujimura,<sup>8</sup> M. Fujiwara,<sup>1,9</sup> S. Fukui,<sup>1</sup> W. Gohn,<sup>10</sup> K. Hicks,<sup>11</sup> A. Hosaka,<sup>1</sup> T. Hotta,<sup>1</sup> S. H. Hwang,<sup>12</sup> K. Imai,<sup>13</sup> T. Ishikawa,<sup>14</sup> K. Joo,<sup>10</sup> Y. Kato,<sup>15</sup> Y. Kon,<sup>1</sup> H. S. Lee,<sup>16</sup> Y. Maeda,<sup>17</sup> T. Mibe,<sup>18</sup> M. Miyabe,<sup>14</sup> Y. Morino,<sup>18</sup> N. Muramatsu,<sup>14</sup> T. Nakano,<sup>1</sup> Y. Nakatsugawa,<sup>18,19</sup> S. i. Nam,<sup>20</sup> M. Niiyama,<sup>21</sup> H. Noumi,<sup>1</sup> Y. Ohashi,<sup>7</sup> T. Ohta,<sup>1,22</sup> M. Oka,<sup>1</sup> J. D. Parker,<sup>21,23</sup> C. Rangacharyulu,<sup>24</sup> S. Y. Ryu,<sup>1</sup> T. Sawada,<sup>2,25</sup> H. Shimizu,<sup>14</sup> E. A. Stokovskiy,<sup>26,1</sup> Y. Sugaya,<sup>1</sup> M. Sumihama,<sup>27</sup> T. Tsunemi,<sup>21</sup> M. Uchida,<sup>28</sup> M. Ungaro,<sup>10</sup> S. Y. Wang,<sup>2,29</sup> and M. Yosoi<sup>1</sup>

(LEPS Collaboration)

<sup>1</sup>Research Center for Nuclear Physics, Osaka University, Ibaraki, Osaka 567-0047, Japan

<sup>2</sup>Institute of Physics, Academia Sinica, Taipei 11529, Taiwan

<sup>3</sup>Department of Physics, National Central University, Taoyuan City 32001, Taiwan

<sup>4</sup>RIKEN Nishina Center, 2-1 Hirosawa, Wako, Saitama 351-0198, Japan

<sup>5</sup>Department of Physics, Korea University, Seoul 02841, Republic of Korea

<sup>6</sup>Light Source Division, National Synchrotron Radiation Research Center, Hsinchu, 30076, Taiwan

<sup>7</sup>Japan Synchrotron Radiation Research Institute, Sayo, Hyogo 679-5143, Japan

<sup>8</sup>Wakayama Medical College, Wakayama, 641-8509, Japan

<sup>9</sup>National Institutes for Quantum and Radiological Science and Technology, Tokai, Ibaraki 319-1195, Japan

<sup>10</sup>Department of Physics, University of Connecticut, Storrs, CT 06269-3046, USA

<sup>11</sup>Department of Physics and Astronomy, Ohio University, Athens, Ohio 45701, USA

<sup>12</sup>Korea Research Institute of Standards and Science (KRISS), Daejeon 34113, Republic of Korea

<sup>13</sup>Advanced Science Research Center, Japan Atomic Energy Agency, Tokai, Ibaraki 319-1195, Japan

<sup>14</sup>Research Center for Electron Photon Science, Tohoku University, Sendai, Miyagi 982-0826, Japan

<sup>15</sup>Kobayashi-Maskawa Institute, Nagoya University, Nagoya, Aichi 464-8602, Japan

<sup>16</sup>Rare Isotope Science Project, Institute for Basic Science, Daejeon 34047, Korea

<sup>17</sup>Proton Therapy Center, Fukui Prefectural Hospital, Fukui 910-8526, Japan

<sup>18</sup>High Energy Accelerator Organization (KEK), Tsukuba, Ibaraki 305-0801, Japan

<sup>19</sup>Institute of High Energy Physics, Chinese Academy of Sciences, Beijing 100049, China

<sup>20</sup>Department of Physics, Pukyong National University (PKNU), Busan 608-737, Republic of Korea

<sup>21</sup>Department of Physics, Kyoto University, Kyoto 606-8502, Japan

<sup>22</sup>Department of Radiology, The University of Tokyo Hospital, Tokyo 113-8655, Japan

<sup>23</sup>Neutron Science and Technology Center, Comprehensive Research

Organization for Science and Society (CROSS), Tokai, Ibaraki 319-1106, Japan

<sup>24</sup>Department of Physics and Engineering Physics, University of Saskatchewan, Saskatoon, SK S7N 5E2, Canada

<sup>25</sup>Physics Department, University of Michigan, Michigan 48109-1040, USA

<sup>26</sup>Joint Institute for Nuclear Research, Dubna, Moscow Region, 142281, Russia

<sup>27</sup>Department of Education, Gifu University, Gifu 501-1193, Japan

<sup>28</sup>Department of Physics, Tokyo Institute of Technology, Tokyo 152-8551, Japan

<sup>29</sup>ChemMatCARS, The University of Chicago, Argonne, Illinois 60439, USA

(Dated: December 10, 2021)

Differential cross sections and photon-beam asymmetries for the  $\bar{\gamma}p \rightarrow \pi^- \Delta^{++}(1232)$  reaction have been measured for  $0.7 < \cos \theta_{\pi^-}^{c.m.} < 1$  and  $E_\gamma=1.5-2.95$  GeV at SPring-8/LEPS. The first-ever high statistics cross-section data are obtained in this kinematical region, and the asymmetry data for  $1.5 < E_\gamma(\text{GeV}) < 2.8$  are obtained for the first time. This reaction has a unique feature for studying the production mechanisms of a pure  $u\bar{u}$  quark pair in the final state from the proton. Although there is no distinct peak structure in the cross sections, a non-negligible excess over the theoretical predictions is observed at  $E_\gamma=1.5-1.8$  GeV. The asymmetries are found to be negative in most of the present kinematical regions, suggesting the dominance of  $\pi$  exchange in the  $t$  channel. The negative asymmetries at forward meson production angles are different from the asymmetries previously measured for the photoproduction reactions producing a  $d\bar{d}$  or an  $s\bar{s}$  quark pair in the final state. Advanced theoretical models introducing nucleon resonances and additional unnatural-parity exchanges are needed to reproduce the present data.

PACS numbers: 13.60.Le, 14.20.Gk, 14.40.Be, 14.70.Bh, 25.20.Lj

The photoproduction of a  $d\bar{d}$  quark pair and an  $s\bar{s}$  quark pair in the final state has been extensively studied by the  $\gamma p \rightarrow \pi^+ n$  [1–3] and  $\gamma p \rightarrow K^+ \Lambda$  and  $K^+ \Sigma^0$  [4–11] reactions, respectively. However, the production

of a  $u\bar{u}$  quark pair in the final state has not been well studied. Although the production of a  $\pi^0$  meson, with a quark-model wavefunction of  $(u\bar{u} - d\bar{d})/\sqrt{2}$ , or  $\eta$  meson, with a wavefunction of  $(u\bar{u} + d\bar{d} + s\bar{s})/\sqrt{3}$ , includes the  $u\bar{u}$

quark-pair production, an exclusive study of a pure  $u\bar{u}$  quark-pair production is desired. The  $\gamma p \rightarrow \pi^- \Delta^{++}$  reaction is a unique channel to study the photoproduction mechanism of a pure  $u\bar{u}$  quark pair in the final state from the proton.

In quark models, there exist more nucleon resonances than those experimentally observed so far [12]. Since nucleon resonances have relatively wide widths and are overlapping each other, rich physics observables with a wide angular and energy range are needed to study new resonances. The differential cross sections for the  $\gamma p \rightarrow \pi^- \Delta^{++}$  reaction were measured by SLAC at the higher energies of  $E_\gamma=4, 5, 8, 11,$  and  $16$  GeV [13–15]. At medium energies, there are only scarce existing data taken by SLAC at  $2.8$  GeV [16], by CEA for  $E_\gamma=0.5-1.8$  GeV [17], by LAMP2 for  $E_\gamma=2.4-4.8$  GeV [18], by DESY for  $E_\gamma=0.3-5.8$  GeV [19], and by SAPHIR for  $E_\gamma=1.1-2.6$  GeV [20]. Although the  $\pi^- \Delta^{++}$  final state is one of prospective channels to study new nucleon resonances [12], cross-section data with a wide angular and energy range are missing in the world data set.

Basically, the photon-beam asymmetries are  $+1$  for  $\rho$  exchange and are  $-1$  for  $\pi$  exchange in the  $t$  channel in the case of the  $\vec{\gamma} p \rightarrow \pi^- \Delta^{++}$  reaction, which is the same as the case of the  $\vec{\gamma} p \rightarrow \pi^+ n$  reaction [21]. There were three asymmetry measurements at the forward  $\pi^-$  angles of  $|t| < 0.5$  GeV<sup>2</sup> ( $0.8 < \cos \theta_\pi^{c.m.}$ ) at  $2.8$  GeV,  $4.7$  GeV, and  $16$  GeV by SLAC [16, 22], where  $t$  is the Mandelstam variable defined by  $t=(p_\pi - p_\gamma)^2$ . Although negative asymmetries are suggested by these measurements, the number of the data points is limited and the data have large statistical uncertainties. In contrast, pseudoscalar meson photoproduction of either a  $\pi^+$  or a  $K^+$  has positive asymmetries at the forward meson angles of  $0.6 < \cos \theta_{\pi,K}^{c.m.} < 1$  when the total energy  $W$  is higher than the third nucleon resonance region  $W \sim 1.7$  GeV ( $E_\gamma \sim 1.1$  GeV) [1, 3–8]. The  $\pi^-$  photoproduction data may well have a different reaction mechanism than that of other pseudoscalar mesons. Combining the  $\pi^- \Delta^{++}$  data with the established  $\pi^+$  and  $K^+$  photoproduction data is helpful to achieve a unified understanding of hadron photoproduction.

In this Letter, we present the first-ever high statistics differential cross-section and photon-beam asymmetry data for the  $\vec{\gamma} p \rightarrow \pi^- \Delta^{++}$  reaction at the forward  $\pi^-$  angles of  $0.7 < \cos \theta_\pi^{c.m.} < 1$ . The data obtained over the energy range of  $E_\gamma=1.5-2.95$  GeV, covering most of the nucleon resonance region, enabled us to study both nucleon resonances and hadron photoproduction dynamics.

The experiment was carried out using the LEPS beam line [23] at the SPring-8 facility in Japan. The photon beam was produced by the laser backscattering technique using a deep-UV laser with a wavelength of  $257$  nm [24]. The energy range of tagged photons was from  $1.5$  to  $2.96$  GeV. The laser light was polarized linearly with a polarization degree of  $98\%$ . The polarization of tagged photons was  $88\%$  at  $2.96$  GeV and was  $28\%$  at  $1.5$  GeV [25].

The photon beam was incident on a liquid hydrogen target (LH<sub>2</sub>) with a length of  $16$  cm.

Charged particles emitted from the LH<sub>2</sub> target were detected at forward angles by using the LEPS spectrometer. The aerogel Cherenkov counter was not used, and electrons or positrons were vetoed using a plastic scintillation counter installed at the downstream position of the three drift chambers. For the details about the LEPS spectrometer, see Refs. [4, 23, 25].

Events with a  $\pi^-$  meson were identified from its mass within  $3\sigma$  where  $\sigma$  is the momentum dependent mass resolution and was measured to be  $60$  and  $110$  MeV/ $c^2$  for  $1$  and  $2$  GeV/ $c$  momentum pions, respectively. The events from the LH<sub>2</sub> target were selected by a cut on the  $z$ -vertex distribution. Contamination events from the start counter, placed downstream of the target, were  $0.5\%$  at most.

Figure 1 shows the missing-mass spectra for the  $\gamma p \rightarrow \pi^- X$  reaction. The  $\Delta^{++}(1232)$  peaks are clearly observed at  $1.23$  GeV/ $c^2$ . The contribution from electrons, mainly originating from the  $e^+e^-$  pair creation, is observed for  $0.966 < \cos \theta_\pi^{c.m.} < 1$ . The number of  $\pi^- \Delta^{++}$  events was about  $400$  k in total.

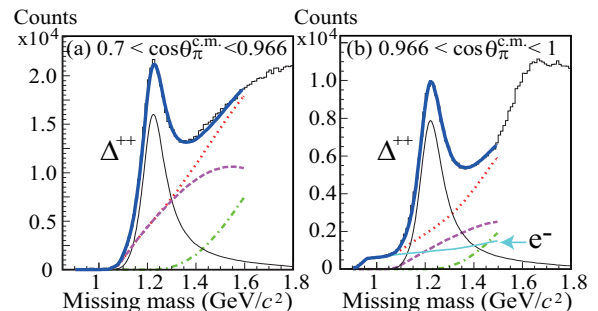


FIG. 1. Missing-mass spectra for the  $\gamma p \rightarrow \pi^- X$  reaction for  $E_\gamma=1.5-2.95$  GeV. The thick solid curves (blue) are the results of the fits, and the thin solid curves (black) are the  $\Delta^{++}$  contributions. The dotted curves (red) are the total contribution from backgrounds. The dashed (purple) and dotted-dashed (green) curves are the contributions from  $\rho/2\pi$  and  $3\pi$  productions, respectively. The curve (light blue) indicated by the arrow is the contribution from the electron background.

The  $\gamma p \rightarrow \pi^- \Delta^{++}$  reaction events were selected by fitting a missing-mass spectrum with curves for the  $\Delta^{++}$  peak,  $\rho$ ,  $2\pi$ ,  $3\pi$  productions, and electron background based on GEANT simulations. For the  $\rho$ -meson productions, the differential cross sections and decay angular distributions in Ref. [20] were assumed, and the multipion productions according to Lorentz-invariant Fermi phase space were performed for the  $2\pi$  and  $3\pi$  productions. The electron background events were generated to reproduce the momentum distributions of the real data. The number of adjustable parameters in the fit was  $5$  in total. No interference between the  $\pi^- \Delta^{++}$  and other reactions was assumed in this analysis using single  $\pi^-$  events. The shape of the  $\Delta^{++}(1232)$  was assumed to be

given by a Jackson relativistic Breit-Wigner form [14, 26],

$$B(m) \propto \frac{m_0 \Gamma(m)}{(m^2 - m_0^2)^2 + m_0^2 \Gamma^2(m)}, \quad (1)$$

with

$$\Gamma(m) = \Gamma(m_0) \left(\frac{q}{q_0}\right)^3 \left(\frac{am_\pi^2 + q_0^2}{am_\pi^2 + q^2}\right) \left(\frac{m_0}{m}\right), \quad (2)$$

where  $m_0 = 1.232$  GeV,  $\Gamma(m_0) = 0.117$  GeV,  $a = 2.2$ , with  $q(q_0)$  being the c.m.-system momentum at masses  $m(m_0)$  in the  $\Delta^{++}$  rest system. As a result of the fit, the  $\Delta^{++}$  yield for the relativistic Breit-Wigner form (including the tail) was obtained for each incident photon energy and angular bin. The acceptance of the LEPS spectrometer for  $\pi^-$  mesons was obtained by the GEANT simulations. The differential cross sections for the  $\pi^- \Delta^{++}$  reaction were obtained by using the same method described in Ref. [4]. The LEPS spectrometer has almost the same acceptance for the  $\pi^-$  and  $\pi^+$  mesons, and the cross sections for the  $\gamma p \rightarrow \pi^+ n$  reaction [1] obtained from the same data set agree well with the data obtained by CLAS [2] and DESY [27].

Figure 2 shows the differential cross sections for the  $\gamma p \rightarrow \pi^- \Delta^{++}$  reaction as a function of  $E_\gamma$ . The cross sections decrease rapidly with increasing photon energy for  $0.7 < \cos \theta_\pi^{c.m.} < 0.933$ . The energy dependence of the cross sections is small for  $0.966 < \cos \theta_\pi^{c.m.} < 1$ . There is no distinct peak structure in the cross sections. The cross sections increase rapidly when the  $\pi^-$  angle becomes smaller. A strong forward peaking of the cross sections is observed. Similar strong forward peaking at  $|t| < 0.2$  GeV<sup>2</sup> was reported for  $E_\gamma = 5, 8, 11,$  and  $16$  GeV by SLAC [14]. The momentum transfer of  $|t| < 0.2$  GeV<sup>2</sup> corresponds to the  $\pi^-$  angular region of  $0.9 < \cos \theta_\pi^{c.m.} < 1$  in the present experiment. The exchange of an isospin  $I = 1$  meson ( $\pi$  or  $\rho$ ) in the  $t$  channel is expected to be the dominant reaction mechanism in the present kinematical region. Since the  $\rho$ -meson exchange contribution becomes weak at forward  $\pi$  angles in pion photoproduction [21],  $\pi$ -meson exchange is inferred to play an important role in making the forward-peaking  $\pi^- \Delta^{++}$  cross sections for  $0.9 < \cos \theta_\pi^{c.m.} < 1$ .

The LEPS cross sections for the  $\pi^- \Delta^{++}$  reaction are in good agreement with the cross sections measured by DESY [19] and SLAC [16] overall. The LEPS cross sections also agree well with those measured by LAMP2 [18] except for  $0.966 < \cos \theta_\pi^{c.m.} < 1$ . The cross sections by SAPHIR [20] agree with the LEPS data for  $0.7 < \cos \theta_\pi^{c.m.} < 0.933$  and are smaller than the LEPS data for  $0.933 < \cos \theta_\pi^{c.m.} < 0.966$ . Since the  $\pi^- \Delta^{++}$  reaction has strong forward-peaking cross sections, small differences in the  $\pi^-$  angular regions between the SAPHIR and present data might cause these disagreements.

Theoretical calculations, employing the tree-level Regge-Born interpolation model without nucleon resonance contributions by S. i. Nam [28], almost reproduce the present cross sections. Although the cutoff mass parameter was optimized from 450 MeV to 500 MeV to fit

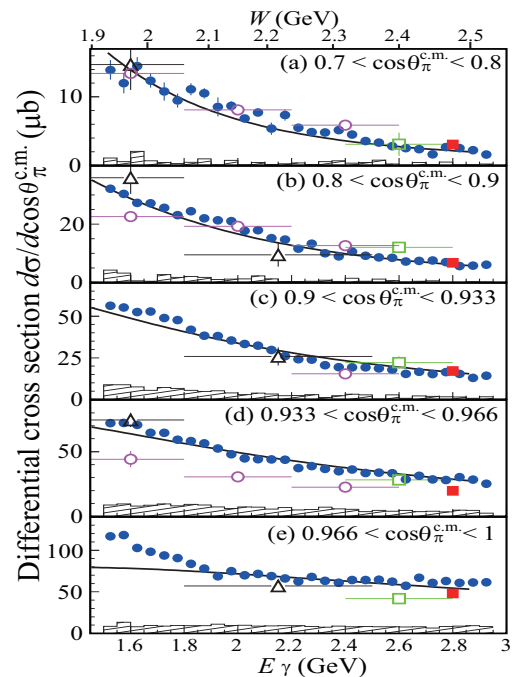


FIG. 2. Differential cross sections for the  $\gamma p \rightarrow \pi^- \Delta^{++}$  reaction as a function of  $E_\gamma$ . The closed circles, open circles, open triangles, open squares, and closed squares are the data obtained by LEPS, SAPHIR [20], DESY [19], LAMP2 [18], and SLAC [16], respectively. Since the data obtained by the other groups had the form  $d\sigma/dt$ , they were transformed to the form  $d\sigma/d\cos\theta_\pi^{c.m.}$  for the comparison. The hatched histograms are the systematic uncertainties due to the selection of the  $\Delta^{++}$  shape. The solid curves are the results of theoretical calculations by S. i. Nam [28].

the data, the energy dependence of the cross sections for  $0.9 < \cos \theta_\pi^{c.m.} < 1$  and  $E_\gamma = 1.5-1.8$  GeV was not reproduced. One of the possible explanations for this discrepancy can be attributed to the absence of resonance contributions in the theory. For instance,  $N^*(1900, 3/2^+)$ , which strongly couples to  $\pi\Delta$ , could be responsible for describing a bump observed in the cross section data. Since the  $s$ -channel structures observed in the SAPHIR total cross sections [20] seem to continue up to  $E_\gamma \sim 2$  GeV, the excess in the present cross sections might be the tail of  $s$ -channel structures.

In this analysis, the relativistic Breit-Wigner form in Eq. (1) used by SLAC [14] was employed. Another analysis with a different relativistic Breit-Wigner shape used by DESY [19] gave smaller cross sections than the present cross sections. The differences between the cross sections obtained by the two Breit-Wigner forms are 10% on average and are shown in Fig. 2 as the largest systematic uncertainties. Since both of the relativistic Breit-Wigner shapes originated from the shapes studied by Jackson [26], the differences in shape are not so large. New analyses using different shapes for the  $\rho$ ,  $2\pi$ , and  $3\pi$  production events generated by the simulations with different momentum and angular distributions were per-

formed. The differences between the original and new cross sections were smaller than 10% for most of the data points. Systematic uncertainties of target thickness and photon flux are 1% and 3%, respectively.

The  $\bar{\gamma}p \rightarrow \pi^- \Delta^{++}$  reaction data were measured using vertically and horizontally polarized photons. The photon-beam asymmetry  $\Sigma$  is given as

$$P_\gamma \Sigma \cos 2\phi_\pi = \frac{N_V - N_H}{N_V + N_H}, \quad (3)$$

where  $N_V$  and  $N_H$  are the  $\pi^- \Delta^{++}$  yields with vertically and horizontally polarized photons, respectively, after correcting for the difference of photon flux in both polarizations.  $P_\gamma$  is the polarization of the photons and  $\phi_\pi$  is the  $\pi^-$  azimuthal angle. The  $\pi^- \Delta^{++}$  yield is obtained by fitting a missing-mass spectrum for each  $\phi_\pi$ ,  $\cos \theta_\pi^{c.m.}$ , and  $E_\gamma$  region. Figure 3 shows the ratio  $(N_V - N_H)/(N_V + N_H)$  for the  $\pi^- \Delta^{++}$  reaction events for  $E_\gamma=1.5$ -2.9 GeV.

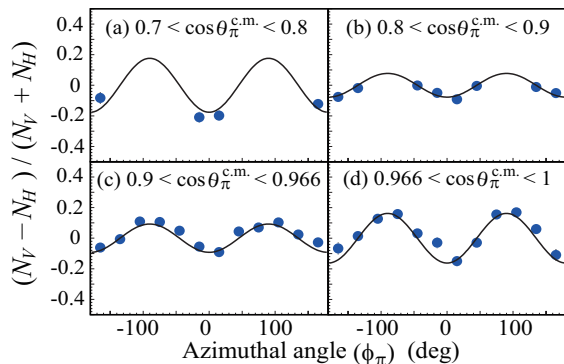


FIG. 3. The ratio  $(N_V - N_H)/(N_V + N_H)$  as a function of  $\pi^-$  azimuthal angle ( $\phi_\pi$ ) for the  $\bar{\gamma}p \rightarrow \pi^- \Delta^{++}$  reaction for  $E_\gamma=1.5$ -2.9 GeV. The curves are the result of the fits with  $P_\gamma \Sigma \cos 2\phi_\pi$ .

Since the LEPS spectrometer has a wide acceptance for the horizontal direction and a narrow acceptance for the vertical direction, the number of events is small at around  $\phi_\pi = \pm 90^\circ$  for  $0.7 < \cos \theta_\pi^{c.m.} < 0.9$ . The ratio  $(N_V - N_H)/(N_V + N_H)$  is large at  $\pm 90^\circ$  and is small at  $0^\circ$  and  $180^\circ$ . The  $\pi^-$  mesons prefer to scatter at  $\phi_\pi$  angles parallel to the polarization plane. The photon-beam asymmetries are therefore negative.

Figure 4 shows the photon-beam asymmetries for the  $\bar{\gamma}p \rightarrow \pi^- \Delta^{++}$  reaction. The systematic uncertainty of the laser polarization is  $\delta\Sigma=0.02$ . The effect of the electron contamination in the  $\pi^-$  sample is removed and that of the start counter contamination in the LH<sub>2</sub> target selection is negligibly small. The limited number of bins for the  $\pi^-$  azimuthal angle in Fig. 3 reduces absolute asymmetry values by 7% on average. The asymmetries obtained using a different relativistic Breit-Wigner shape [19] agree with the present asymmetries. The differences between the two asymmetries are  $\delta\Sigma=0.07$  on average and are shown in Fig. 4 as the largest systematic uncertainties. New analyses using different shapes

for the  $\rho$ ,  $2\pi$ , and  $3\pi$  production events generated by the simulations with different momentum and angular distributions were performed. The differences between the original and new asymmetries were smaller than the statistical errors. For the confirmation of the correctness of the asymmetries, the sideband subtraction analysis using the sideband events of the  $\Delta^{++}$  peak was performed, and the result of this analysis well reproduced the asymmetries in Fig. 4.

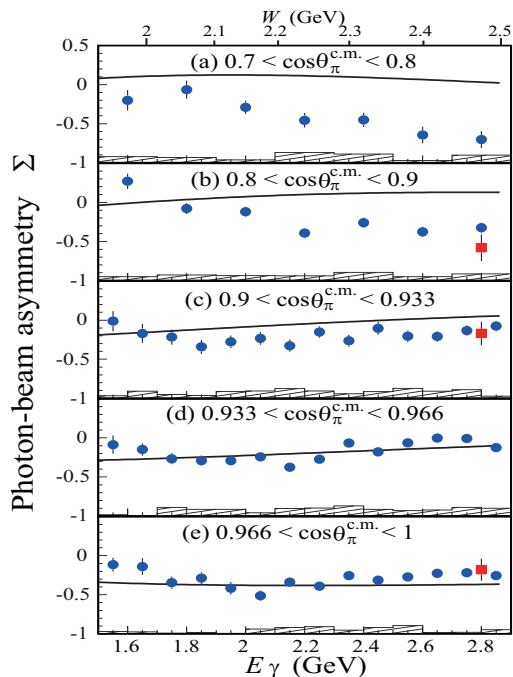


FIG. 4. Photon-beam asymmetries for the  $\bar{\gamma}p \rightarrow \pi^- \Delta^{++}$  reaction as a function of  $E_\gamma$ . The circles and squares are the data obtained by LEPS and SLAC [16], respectively. SLAC measured three asymmetries at  $|t|=0.2$ -0.5, 0.1-0.2, and  $|t_{min}|=0.1$  GeV<sup>2</sup>, and are plotted as squares in (b), (c), and (e). The hatched histograms are the systematic uncertainties due to the selection of the  $\Delta^{++}$  shape. The solid curves are the results of theoretical calculations by S. i. Nam [28].

The asymmetries are found to be negative in most of the LEPS kinematical region, which may be explained by  $\pi$ -meson exchange in the  $t$  channel. The same interpretation is obtained from the strong forward peaking of the cross sections observed in Fig. 2. We have observed positive asymmetries at forward pseudoscalar meson angles in most  $q\bar{q}$  productions in the final state from the proton, such as a  $d\bar{d}$  production with  $\bar{\gamma}p \rightarrow \pi^+ n$  [1, 3] and an  $s\bar{s}$  production with  $\bar{\gamma}p \rightarrow K^+ \Lambda$  and  $K^+ \Sigma^0$  [4–8]. In addition, the photoproduction reactions of neutral pseudoscalar mesons, such as  $\bar{\gamma}p \rightarrow \pi^0 p$  [3, 29] and  $\eta p$  [30, 31], also have positive asymmetries at forward meson production angles. It is quite interesting that only pure  $u\bar{u}$  production in the final state has negative asymmetries. Since preliminary results of the  $\bar{\gamma}p \rightarrow \pi^+ \Delta^0$  reaction show positive asymmetries [32], the production of the spin-parity  $3/2^+$  baryon does not necessarily cause

the negative asymmetries.

SLAC measured three asymmetries at  $E_\gamma=2.8$  GeV [16]. The agreement between the LEPS and SLAC data is reasonable for  $0.9 < \cos\theta_\pi^{c.m.} < 0.933$  and  $0.966 < \cos\theta_\pi^{c.m.} < 1$ . The SLAC data for  $0.8 < \cos\theta_\pi^{c.m.} < 0.9$  is slightly smaller than for the LEPS data.

Since the asymmetry calculated in Ref. [28] has an opposite definition, it is corrected to meet the present definition in Eq. (3). Theoretical calculations by S. i. Nam [28] almost reproduce the negative asymmetry data for  $0.933 < \cos\theta_\pi^{c.m.} < 1$ . As the  $\pi$  angle becomes larger, the calculations predict small positive asymmetries since the  $\pi$ -exchange contribution becomes small. The inconsistency between the data and the calculations becomes large for  $0.7 < \cos\theta_\pi^{c.m.} < 0.9$ . This inconsistency is inferred to be due to the possible existence of a small but finite additional unnatural-parity exchange contribution not taken into account in the theory calculations. Smaller absolute asymmetry values at  $E_\gamma=1.5$ -1.7 GeV and  $0.9 < \cos\theta_\pi^{c.m.} < 1$  might be caused by the bump observed in the cross sections (Fig. 2).

In summary, we have carried out a photoproduction experiment observing the  $\bar{\gamma}p \rightarrow \pi^- \Delta^{++}$  reaction by using linearly polarized tagged photons with energies from 1.5 to 2.95 GeV. Differential cross sections and photon-beam asymmetries have been measured for  $0.7 < \cos\theta_\pi^{c.m.} < 1$ . There is no distinct peak structure in the cross sections. However, a non-negligible excess of the cross sections, possibly due to the tail of nucleon or  $\Delta$  resonances, over the theoretical predictions is observed at  $E_\gamma=1.5$ -1.8 GeV. Strong forward-peaking cross sections, expected from  $\pi$  exchange in the  $t$  channel, are observed. The asymmetries for the  $\pi^- \Delta^{++}$  reaction are found to be neg-

ative in most of the present kinematical regions, which suggests that the  $\pi$  exchange in the  $t$  channel is dominant. The negative asymmetries are unusual in the photoproduction reactions from the proton studied in the past [1, 3–8]. Analogous results were obtained in the measurements of the single-spin asymmetries for the  $pp$  or  $ep$  reactions [33], where inclusive  $\pi^-$  production has negative asymmetries while inclusive  $\pi^+$  and  $K^+$  productions have positive asymmetries. The  $\pi^-$  production is inferred to have a different reaction mechanism from the  $\pi^+$  and  $K^+$  productions. The  $\gamma p \rightarrow \pi^- \Delta^{++}$  reaction data provide a unique chance for studying the  $u\bar{u}$  quark pair production. The combination of these data with the established data for the  $d\bar{d}$  and  $s\bar{s}$  quark pair productions is helpful to achieve unified understanding of the hadron photoproduction.

## ACKNOWLEDGMENTS

The authors gratefully acknowledge the staff of the SPring-8 facility for the supports with excellent experimental conditions. The experiments were performed at the BL33LEP of SPring-8 with the approval of the Japan Synchrotron Radiation Research Institute (JASRI) as a contract beamline (Proposal No. BL33LEP/6001). H.K. thanks Prof. E. Oset, Prof. T. Mart, Prof. S. Kumano, and Prof. H. Kamano for fruitful discussions. This research was supported in part by the Ministry of Education, Science, Sports and Culture of Japan, the National Science Council of the Republic of China, the National Research Foundation of Korea, and the U.S. National Science Foundation.

- 
- [1] H. Kohri *et al.*, Phys. Rev. C **97**, 015205 (2018).
  - [2] M. Dugger *et al.*, Phys. Rev. C **79**, 065206 (2009).
  - [3] M. Dugger *et al.*, Phys. Rev. C **88**, 065203 (2013).
  - [4] M. Sumihama *et al.*, Phys. Rev. C **73**, 035214 (2006).
  - [5] H. Kohri *et al.*, Phys. Rev. Lett. **97**, 082003 (2006).
  - [6] A. Lleres *et al.*, Eur. Phys. J. A **31**, 79 (2007).
  - [7] C. A. Paterson *et al.*, Phys. Rev. C **93**, 065201 (2016).
  - [8] S. H. Shiu *et al.*, Phys. Rev. C **97**, 015208 (2018).
  - [9] R. Bradford *et al.*, Phys. Rev. C **73**, 035202 (2006).
  - [10] M. E. McCracken *et al.*, Phys. Rev. C **81**, 025201 (2010).
  - [11] B. Dey *et al.*, Phys. Rev. C **82**, 025202 (2010).
  - [12] S. Capstick and W. Roberts, Phys. Rev. D **49**, 4570 (1994).
  - [13] R. L. Anderson *et al.*, Phys. Rev. D **14**, 679 (1976).
  - [14] A. M. Boyarski *et al.*, Phys. Rev. Lett. **22**, 148 (1969).
  - [15] A. M. Boyarski *et al.*, Phys. Rev. Lett. **25**, 695 (1970).
  - [16] J. Ballam *et al.*, Phys. Rev. D **5**, 545 (1972).
  - [17] Cambridge Bubble Chamber Group, Phys. Rev. **163**, 1510 (1967).
  - [18] D. P. Barber *et al.*, Z. Phys. C **6**, 93 (1980).
  - [19] ABBHMM Collaboration, Phys. Rev. **175**, 1669 (1968).
  - [20] C. Wu *et al.*, Eur. Phys. J. A **23**, 317 (2005).
  - [21] M. Guidal, J.-M. Laget, M. Vanderhaeghen, Phys. Lett. B **400**, 6 (1997).
  - [22] D.J. Quinn *et al.*, Phys. Rev. D **20**, 1553 (1979).
  - [23] T. Nakano *et al.*, Nucl. Phys. A **684**, 71 (2001).
  - [24] N. Muramatsu *et al.*, Nucl. Instr. Meth. A **737**, 184 (2014).
  - [25] S. H. Hwang, Ph.D. thesis, Pusan National University, 2012 (unpublished).
  - [26] J. D. Jackson, Nuovo Cimento **34**, 1644 (1964).
  - [27] G. Boschhorn *et al.*, Phys. Rev. Lett. **18**, 571 (1967).
  - [28] Seung-il Nam and Byung-Geel Yu, Phys. Rev. C **84**, 025203 (2011).
  - [29] N. Sparks *et al.*, Phys. Rev. C **81**, 065210 (2010).
  - [30] D. Elsner *et al.*, Eur. Phys. J. A **33**, 147 (2007).
  - [31] P. Collins *et al.*, Phys. Lett. B **771**, 213 (2017).
  - [32] H. Kohri, JPS Conf. Proc. **10**, 010008 (2016).
  - [33] C. A. Aidala *et al.*, Rev. Mod. Phys. **85**, 655 (2013).